Numerical model-based analysis of energy-efficient reverse osmosis (EERO) process: Performance simulation and optimization

Kwanho Jeong[a,b], Minkyu Park[c], and Tzyy Haur Chong[a,b,*]

a. School of Civil and Environmental Engineering, Nanyang Technological University, Singapore 639798, Singapore

b. Singapore Membrane Technology Centre, Nanyang Environment and Water Research Institute, Nanyang Technological University, Singapore 637141, Singapore

c. Department of Chemical and Environmental Engineering, University of Arizona, Tucson, AZ 85721, USA

A Manuscript for

DESALINATION

* Corresponding author

E-mail: thchong@ntu.edu.sg (T.H. Chong)

Abstract

We conducted a feasibility study of the energy-efficient reverse osmosis (EERO) process, which is a multi-stage membrane system that integrates single-stage reverse osmosis (SSRO) and a countercurrent membrane cascade with recycle (CMCR). To this end, we developed a numerical model for the 1-2 EERO process (one SSRO stage with two stages in CMCR: one nanofiltration (NF) stage followed by one terminal RO stage), then validated the model using performance data obtained from commercial RO projection software. Retentate recycle ratio was one of the key parameters to determine energy efficiency of EERO. In addition, the implementation of NF membranes in the first stage of CMCR yielded additional improvement in EERO performance and played an important role in determining optimum salt rejection. An optimal design of the NF stage was successfully achieved by hybridization of different NF membranes in a vessel (internally staged design, ISD). Under the conditions optimized, EERO exhibited not only greater energy efficiency (3 – 25%), but lower concentration polarization (CP) and potentials of membrane fouling than conventional SSRO for $\geq$ 55% overall recoveries because of reduced water flux in the lead elements (averagely 34%). These findings can thus provide insight into optimal design and operation of the EERO process.

Keywords

Reverse osmosis; Seawater desalination; Energy-efficient; Multistage processing; Specific energy consumption

1. Introduction

Two major innovations of membrane development are findings of Loeb–Sourirajan asymmetric and thin-film composite membranes [1]. Recently, research for emerging membranes such as those incorporated with aquaporin and nanomaterials including carbon nanotubes have been thrived as a means of membrane performance enhancement, while challenges remain such as limited salt rejection and commercialization [2]. A central dilemma of membrane development is tradeoff relation of water and salt permeabilities, a major hindrance for developing a high-performance membrane with both high water permeability and salt rejections [3]. Meanwhile, process optimization can play an imperative role in reducing energy consumption, therefore lowering the cost of water production. One of the main benefits of process optimization is its facileness to simulate various membrane configurations without implementation of pilot testing, therefore enable to propose various conceptual and energy-efficient membrane process designs.

A single-stage reverse osmosis (SSRO) process, a conventional RO membrane configuration, achieved a high water recovery of ~50% with novel membrane materials and innovative designs of system and membrane module [2]. SSRO has been a preferred design of reverse osmosis (RO) for seawater desalination than two RO stages in series when similar water recovery rate is aimed [4]. This is because reduced energy for two-stage RO membrane does not offset its additional capital cost [2, 4]. Unfortunately, SSRO has also a drawback of being a high recovery process; net driving pressure (NDP) for water permeation is unevenly distributed over the membrane module [4]; NDP is gradually declining along a pressure vessel and it is more exacerbated by increasing either the recovery or the feed concentration at a given recovery [4]. Consequently, an imbalance in water flux accompanies a high degree of thermodynamic irreversibility at lead elements due to membrane fouling, thereby degrading

the energy efficiency of RO process [5, 6]. In this respect, two RO stages in series can reduce the thermodynamic irreversibility of SSRO, nonetheless such configuration design is impractical and not viable for achieving a high recovery of > 60% for desalination of high saline feed water (> 35 g/L TDS) [7], hence generally adopted for brackish water reverse osmosis (BWRO) [8]. This is because osmotic pressure differential (OPD) across membranes and operating pressure at the second stage increase excessively, not allowable for the majority of commercial membranes [7]. For improvement of the existing two-stage SWRO system, the Mega-ton Water System project in Japan can be example. Two-stage high recovery RO membrane system, named Low-Pressure Multi-Stage System (LMS), was recently proposed and can achieve 60% recovery by the reduced pressure of the first stage with a short pressure vessel that contains 2-4 elements for the 1^{st} stage, then followed by a relatively long vessel for the 2^{nd} stage [9]. However, it was evaluated that LMS is also difficult to expect further energy reduction as compared to a conventional system, unless LMS applies high efficiency of the elemental technologies developed in the Mega-ton project: a large-scaled high-pressure pump; a new isobaric ERD; and a low-pressure SWRO membrane [9].

The hybrid and multi-stage systems have recently emerged as a prospective design of RO process to overcome the aforementioned demerits of conventional RO unit configurations [2]. A key common feature of these two systems is to lower the level of OPD in a RO stage, with osmotic dilution of the seawater feed and a staged membrane operation, respectively. Many studies demonstrated the potential of energy reduction for hybrid systems, where forward osmosis (FO) or pressure retarded osmosis (PRO) is combined with RO as a pre-treatment process [10, 11]. Nevertheless, they still have technological barriers for practical implementation due to the lack of commercial membranes suitable for FO and PRO processes [12]. In case of an ideal multi-stage system, the theoretical minimum energy required for

desalination should be close to a thermodynamic limit of concentrates in each stage [2]. This plays a role in reducing the flux imbalance and thermodynamic irreversibility over the vessels of all stages [6]. Lin and Elimelech confirmed the potential of significant energy reduction with the multi-stage systems that employed direct pass and closed-circuit RO configurations [6, 13]. In closed-circuit RO (also known as semi-batch RO), however, the continuous mixing of recirculated brine with the incoming fresh feed can limit (degrade) energy efficiency due to entropy generation inside the system [14]. A fully batch RO, hence, has received great attention recently, since it employs a non-pressurized mixing tank to minimize a differential in concentrations of two solutions fed to membrane module, and thereby further reduce energy consumption over semi-batch RO [14]. Nevertheless, these kind of multi-stage systems would be still challenging to be practically implemented due to that: one may need large numbers of stages over eight (theoretically infinite stages) to avoid substantial increases in the OPD and feed pressure required for downstream stages, similar to the two stages in series as described earlier; the others (batch/semi-batch RO) would need robust pumps and ERDs in which the high efficiencies are continuously maintained under operation with continually varying hydraulic pressures [15], and require further development of system operation, such as temporary pressure control to maintain decent recovery during recirculation of the brine back to the feed water [13]. There has been little to no operational experience of a fully batch RO process [15].

A promising membrane system design was conceptually proposed by Chong et al.: energy-efficient reverse osmosis (EERO) [7]. The EERO process was configured as multiple stages that incorporate one or more SSRO stages and a countercurrent membrane cascade with recycle (CMCR). In the EERO process, the brine from SSRO is further processed by the CMCR which consists of one or more nanofiltration (NF) stages and a terminal RO stage. This concept

was proposed based on optimization strategy for multistage processing with recycling of one or both counter-currently flowing streams (e.g., distillation) [7]. A key feature of CMCR is to lower the OPD across membrane by using (i) NF membrane to allow passage of more salts with water than RO membrane, and (ii) interstage recycling [8]: permeate recycle from the first to subsequent stages; retentate recycle from the last to preceding stages. As a result, the EERO process can achieve a reduction in ~33% in the OPD relative to conventional SSRO configuration, and thus enhance a water recovery at the same quantity of specific energy consumption (SEC) since the reduced energy of 33% is used for producing additional water in CMCR [7]. However, in some cases, EERO energy efficiency was reported to be lower than conventional RO designs, alluding necessity of EERO optimization [16].

In previous studies [7, 16], the analytical models, solving a set of algebraic equations, facilitated assessment of the EERO performance with a few system design variables: water recovery and efficiency of ancillary equipment such as energy recovery device (ERD) and booster pumps (BPs). While the previous studies succeeded to conceptually prove the feasibility of EERO, their analytical model has limitations that need to be addressed. For instance, an ideal membrane module that can operate at the thermodynamic limit ($\Delta p = \Delta\pi$) was assumed. Moreover, concentration polarization (CP) and pressure drop along the flow channel due to frictional losses were not taken into account [7, 16], which plays more important roles to determine energy efficiency for systems with higher water recovery [8] and larger scale such as multistage processes. Specifically, operation with a higher recovery causes a high membrane flux, thereby enhancing CP. In addition, many stages (i.e., longer flow channel) can increase the degree of pressure drop. These two phenomena result in the reduced net driving pressure (NDP) for permeate flux across membrane. Their disregard, therefore, inevitably incurs the overestimation of the EERO system performance. Furthermore, the previous model

did not embody the properties of specific membranes, so that it may be infeasible to reflect realistic conditions of operation (i.e., dependent strongly on membrane properties) in simulation; for instance, as the rejection of NF membrane was not specified in the previous, it is a challenge to find suitable membranes to satisfy the required rejection.

The primary aims of this study are to 1) develop a numerical model for a 1-2 EERO process that consists of one SSRO stage and two stages in CMCR, and subsequently 2) assess energy efficiency of the EERO process, and finally 3) determine optimal conditions for retentate recycle ratio, water recovery rate, and NF module design by hybridization of different NF membranes. CP and pressure drop across a pressure vessel were incorporated in the numerical model in order to realistically simulate transport phenomena. In addition, SEC of the EERO process was compared with conventional SSRO system under various conditions of overall water recovery. This would provide valuable information on acceptable treatment capacity of the EERO process, in terms of electrical operating cost. This study was intended not only to provide optimal design and operating conditions of the EERO process, but also to address a controversial issue regarding applicability of the EERO system for seawater desalination.

2. Modeling procedure

2.1. Process description

Fig. 1 illustrates the configuration of a 1-2 EERO process. This multi-stage system is comprised of a SSRO stage and a two-stage CMCR containing one NF stage and one RO stage. In Stage 1 of CMCR, the retentates (brines) from SSRO stage and recycled from terminal RO stage in CMCR are treated by NF membrane. This plays an influential role in reducing the OPD

for the CMCR stages by NF membrane passing more salt with water than RO membrane. In Stage 2 of CMCR, the permeate from Stage 1 is desalinated using RO membrane to improve the purity and recovery of the water product. Furthermore, the NF interstage can remove large portion of divalent ions in the first stage RO brine, allowing for lower saturation indexes in comparison with two (or multiple) RO stages in series. It will also be operating at lower salinities in the recirculation step, which potentially could improve the salt rejection slightly.

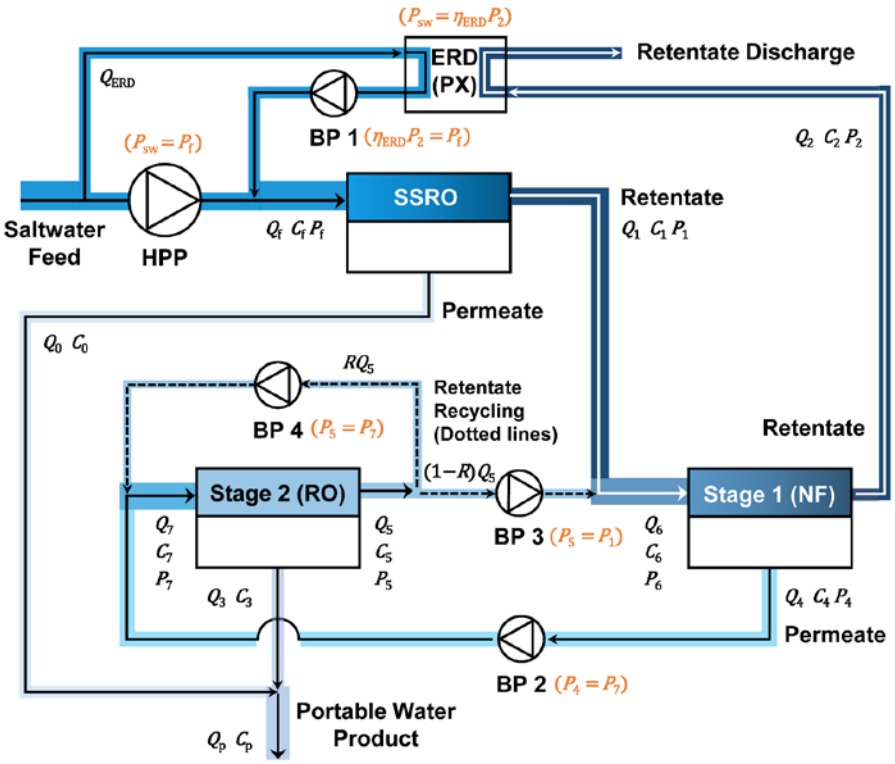

Fig. 1. A schematic of energy-efficient reverse osmosis (EERO) process where single-stage reverse osmosis (SSRO) is combined with a countercurrent membrane cascade with recycle (CMCR). In the example is a 1-2 EERO, where the CMCR consists of two stages; one nanofiltration (NF) stage and one terminal reverse osmosis (RO) stage.

It is generally recognized that most of the commercial NF membranes are not designed to be operated at high pressure, for example NF90 from Dow FilmTec, the recommended

pressure limit is 41 bars. For salty water treatment purpose, however, some of commercially available NF membranes can be operated up to a maximum pressure of 83 bar [17]. In this simulation work, we have assumed that the membrane can be operated at higher pressure i.e. up to 69 bar similar to typical RO and the membrane performance is not compromised. Also, from the pilot test conducted for a 1-2 EERO process, the NF membrane can be operated at pressure higher than 41 bars; the results from the pilot test will be reported in a forthcoming paper. Of all streams at Stage 1, the permeate stream is pressurized by an interstage booster pump (BP 2) and fed into Stage 2 (RO). Meanwhile, the hydraulic energy of NF retentate (i.e., final retentate of EERO process) is recovered by an ERD. This is an additional energy source to pressurize a partial amount of the feed to the SSRO stage, although a booster pump (BP 1) consumes the energy to equalize the feed pressure discharged from the ERD with that from a high-pressure pump (HPP). In the Stage 2, the retentate is split into two recycle streams (dotted lines in Fig. 1), and combined with the brine stream of SSRO and feed stream of Stage 2, respectively. These recycled streams are elevated by BP 3 and BP 4 to make their pressures equal to those of the main feed to Stage 1 and Stage 2 (solid lines in Fig. 1). This retentate recycle not only enriches the feed water quantity to Stage 1 and Stage 2, but also has a dilution effect on the highly concentrated retentate from the SSRO stage. Accordingly, it can diminish the degree of the OPD for the subsequent stages.

The 1-2 EERO is a process with “semi-closed loop recycling” unlike semi-batch RO with “full-closed loop recycling” (commonly known as closed-circuit desalination). This is because permeate and retentate streams in CMCR are simultaneously and continuously discharged in an open-loop manner from the point of view of the whole process, while its individual stages are running in a closed-loop manner. The EERO, therefore, would incur an entropy-of-mixing penalty smaller than the semi-batch RO. The mixing of two different

concentration solutions itself may not crucial for entropy generation, but continuous accumulation of salt within the system where at least one of outlet streams is (fully or partially) recycled to the inlet feed stream. This is one of main issues of degraded energy efficiency in the semi-batch RO: salt remains until the brine is moved out of the system throughout closed recirculation loops of the brine, thereby causing gradual increases in osmotic pressure in the feed and operating pressure. A series of such (salt) cumulative progress due to closed-loop recycling and mixing can lead to significant entropy generation and thereby entropic energy loss.

2.2. System performance

2.2.1 Inlet feed water to CMCR stages

Differential mass balance Eqs. (1) – (4) were employed to quantify the feed water variables, Q_6, C_6, Q_7, and C_7, under steady-state conditions. Due to mixing of feed and recycled retentate (brine) streams of different salinities for CMCR stages, those variables change with time, but become stationary after certain period (or cycles) of transient behavior. As discussed in the preceding section, CMCR itself is a semi-closed loop process unlike a full-closed loop process such as batch or semi-batch RO. Eqs. (1) – (4) were derived based on conservation laws and several assumptions: complete mixing of two different fluid streams; negligible hydraulic residence time within stages and pipelines.

$$\frac{\mathrm{d}V_6}{\mathrm{d}t} = Q_1 + \left(1-R\right)Q_5 \tag{1}$$

$$\frac{\mathrm{d}C_6}{\mathrm{d}t} = \frac{Q_1 C_1 + (1-R) Q_5 C_5}{V_6} - \frac{C_6}{V_6}\frac{\mathrm{d}V_6}{\mathrm{d}t} \tag{2}$$

$$\frac{\mathrm{d}V_7}{\mathrm{d}t} = Q_4 + RQ_5 \tag{3}$$

$$\frac{\mathrm{d}C_7}{\mathrm{d}t} = \frac{Q_4 C_4 + RQ_5 C_5}{V_7} - \frac{C_7}{V_7}\frac{\mathrm{d}V_7}{\mathrm{d}t} \tag{4}$$

where V, Q, and C are the volume, volumetric flow rate, and solute concentration of the fluid, respectively. R is the retentate recycle ratio in Stage 2. Note that hydraulic pressures, P_6 and P_7, are gauge values and constant by adjusting the pressure of two recycle streams using BP 3 and BP 4.

2.2.2 Specific energy consumption

The SEC for 1-2 EERO process can be defined as the ratio of the net rate of work done by main and ancillary equipment to the total flow rate of the water product, given by:

$$\mathrm{SEC}_{\mathrm{EERO}} = \frac{\dot{W}_{\mathrm{HPP}} + \dot{W}_{\mathrm{BP1}} + \left(\dot{W}_{\mathrm{BP2}} + \dot{W}_{\mathrm{BP4}}\right) + \dot{W}_{\mathrm{BP3}}}{Q_{\mathrm{p}}} \tag{5}$$

where Q_{p} is the total permeate flow rate, which is the sum of permeate flow rates of SSRO stage and Stage 2 (Q_0 and Q_3). $\mathrm{SEC}_{\mathrm{EERO}}$ is normalized with respect to the feed osmotic pressure to individual stages, defined as $\mathrm{SEC}_{\mathrm{norm}} = \mathrm{SEC}/\pi_0$ [18]. The work-rate $\dot{W}$ for individual

198 equipment is calculated as follows [18]:

199

200 $$\dot{W}_{\mathrm{HPP}} = \frac{P_{\mathrm{f}}\left(Q_{\mathrm{f}} - Q_2\right)}{\eta_{\mathrm{pump}}} \quad (6)$$

201 $$\dot{W}_{\mathrm{ERD}} = \eta_{\mathrm{ERD}} P_2 Q_2 \quad (7)$$

202 $$\dot{W}_{\mathrm{BP1}} = \frac{\left(P_{\mathrm{f}} - \eta_{\mathrm{ERD}} P_2\right) Q_2}{\eta_{\mathrm{pump}}} \quad (8)$$

203 $$\dot{W}_{\mathrm{BP2}} + \dot{W}_{\mathrm{BP4}} = \frac{P_7\left(Q_7 - K_{\mathrm{STG2}} R Q_5\right)}{\eta_{\mathrm{pump}}} \quad (9)$$

204 $$\dot{W}_{\mathrm{BP3}} = \frac{\left(P_1 - P_5\right)\left(1 - R\right) Q_5}{\eta_{\mathrm{pump}}} \quad (10)$$

205

206 where $\dot{W}_{\mathrm{HPP}}$, $\dot{W}_{\mathrm{ERD}}$, $\dot{W}_{\mathrm{BP1}}$, $\dot{W}_{\mathrm{BP2}}$, $\dot{W}_{\mathrm{BP3}}$, and $\dot{W}_{\mathrm{BP4}}$ refer to the work-rate done by HPP, ERD, BP
207 1, BP 2, BP 3, and BP 4. Note that the two streams in the ERD are assumed to have the same
208 flow rate ($Q_{\mathrm{ERD}} = Q_2$). Eq. (10) is used for $P_5 < P_6$, whereas $\dot{W}_{\mathrm{BP3}}$ is zero for $P_5 \geq P_6$ because BP
209 3 is unnecessary under that condition. P_{f} and Q_{f} are the inlet feed pressure and flow rate,
210 respectively. η_{pump} and η_{ERD} are the efficiencies of pumps and ERD (assumed to be 85% and
211 90%, respectively). K_{STG2} denotes the coefficient to account for the pressure difference between
212 inlet (feed) and outlet (retentate) of the RO membrane module for Stage 2. It can be determined
213 as the ratio of P_5 to P_7. In addition, it should be noted that SEC for conventional SSRO process,
214 $\mathrm{SEC}_{\mathrm{SSRO}}$, is expressed as $(\dot{W}_{\mathrm{HPP}} + \dot{W}_{\mathrm{BP1}})/Q_{\mathrm{p}}$. For the calculation of $\mathrm{SEC}_{\mathrm{SSRO}}$, P_2 and Q_2 of Eq.
215 (6) to (8) are replaced by P_1 and Q_1, respectively.

2.2.3 RO and NF membrane modules

The water and salt transport of RO and NF membranes can be described by irreversible thermodynamics [19]. The Kedem–Katchalsky (KK) model (Eqs. (11) and (12)) were used to determine the water and salt fluxes, J_w and J_s, in pressure-driven membrane processes [20]. The KK model can facilitate modeling of both RO and NF membranes since it has two phenomenological terms accounting for diffusion and convection, while the solution–diffusion model interprets the membrane transport with diffusion [21]. In addition, the KK model is adequate for simply describing the transport of single solute and solvent through the membrane [22], in comparison to other transport models; the Nernst-Planck model and the Donnan–steric–pore model (DSPM), which consider specific transport mechanisms characterized by the electrical and structural properties of the membrane [23]. For RO mode, it was assumed that reflection coefficient, σ, is equal to 1 because diffusion is a dominant mass-transfer process within RO membranes. In contrast, NF membranes are governed by both of diffusion and convection, so that the σ value was set to $0 < \sigma < 1$ because it is correlated with the feed solute concentration [19, 24].

$$J_w = L_p(\Delta p - \sigma\Delta\pi) \tag{11}$$

$$J_s = P_s\Delta c + (1-\sigma)J_w\bar{c} \tag{12}$$

where L_p and P_s are the water and solute permeabilities of the membrane, respectively. Δp and $\Delta\pi$ are the trans-membrane hydraulic and osmotic pressures, respectively. $\Delta\pi$ can be expressed

by the modified van't Hoff equation [25]: $\Delta\pi = (N_{ion}R_gT\Delta c)/M_s$; Δc is the solute concentration difference across the membrane (i.e., $c_m - c_p$). N_{ion}, R_g, T, and M_s denote the number of ions, the ideal gas constant, the absolute temperature, and the molecular weight of the solute, respectively. The average concentration across the membrane, $\bar{c}$, is calculated as the logarithmic mean of c_m and c_p. To consider local variations in the true (real) rejection of solute at different flow rates along membrane channel, we employed Eq. (13), which was derived from the Spiegler–Kedem model suitable for large volume flux and high concentration gradient processes such as RO and NF membranes [26].

$$R_s = 1 - \frac{c_p}{c_m} = \frac{\sigma(1 - F_s)}{1 - \sigma F_s} \tag{13}$$

where F_s is the driving force exerted by solutes and defined as $F_s = \exp[-J_w(1-\sigma)/P_s]$ [22]. The membrane wall concentration, c_m, can be determined using the film theory model [27]: $(c_m - c_p)/(c_b - c_p) = \exp(J_w/k)$; c_p is the permeate concentration, calculated as (J_s/J_w), and c_b is the feed (bulk) concentration. The c_m for reverse osmosis process was estimated with the assumption of complete solute rejection, unlike nanofiltration. The solute mass-transfer coefficient k can be defined as $k = D\cdot\mathrm{Sh}/d_h = a\cdot\mathrm{Re}^b\mathrm{Sc}^c$ [28]. The Sherwood number Sh correlates with the Reynolds number Re ($= \rho\cdot d_h\cdot u_x/\mu$) and the Schmidt number Sc ($= v/D$); D is the solute diffusivity and d_h is the hydraulic diameter of the flow channel; The parameters ρ, μ, and v indicate the density, dynamic viscosity, and kinematic viscosity of the bulk solution, respectively. The constants a, b, and c were set to 0.065, 0.875, and 0.25, respectively, which were empirically obtained for spacer-filled channels [28]. Using Eqs. (14) – (16), we

considered the spatial variations in local fluid properties inside the flow channel. It allows a more accurate prediction for the water and solute fluxes in a full-scale membrane module. The cross-flow velocity u_x, solute concentration c_x, and trans-membrane hydraulic pressure Δp_x at an arbitrary spatial point can be described by [29, 30]:

$$u_x = u_0 - \frac{2}{\varepsilon_{sp}} \int_{x=0}^{x=L} \frac{J_w}{H} \mathrm{d}x \tag{14}$$

$$c_x = \frac{1}{u_x} \left[u_0 c_0 - \frac{2}{\varepsilon_{sp}} \int_{x=0}^{x=L} \frac{J_s}{H} \mathrm{d}x \right] \tag{15}$$

$$\Delta p_x = \Delta p_0 - \frac{12 K \mu}{H^2} \int_{x=0}^{x=L} u_x \mathrm{d}x \tag{16}$$

where u_0, c_0, and Δp_0 are the solute concentration, cross-flow velocity, and trans-membrane hydraulic pressure at the inlet port ($x = 0$), respectively. ε_{sp} is the effective porosity of the flow channel [30]. H and L are the flow channel height and length, respectively. K is the friction coefficient for the channel wall and spacer [29]. The permeate flow rate and concentration for single membrane module are described by:

$$Q_{module}^{p} = \int_{x=0}^{x=TL} J_w W \, \mathrm{d}x \tag{17}$$

$$C_{module}^{p} = \frac{\int_{x=0}^{x=TL} J_w c_p W \, \mathrm{d}x}{Q_{module}^{p}} \tag{18}$$

where TL denotes the total length of a series of membrane elements in a pressure vessel. W is the width of the flow channel. The fractional water recovery for individual and all modules was defined as the ratio of permeate flow rate to feed flow rate: $Y_{SSRO} = Q_0/Q_f$; $Y_{NF} = Q_4/Q_6$; $Y_{RO} = Q_3/Q_7$; $Y_{overall} = (Q_0 + Q_3)/Q_f$ (see Fig. 1).

2.3 Numerical solution of equations

MATLAB software (version. R2017a) was used to compute approximate solutions of the governing Eqs. (1) – (18). For model-based simulation of the 1-2 EERO process, we employed a numerical algorithm, illustrated in Fig. 2:

(1) Physical and physicochemical variables and parameters, regarding operating conditions, feed water, module, and membrane, are inputted (summarized in Table 1).

(2) The performance of each individual stage is obtained by computing the spatial distribution of water and solute transports for RO and NF membrane modules. It can be carried out by employing a finite difference approximation, used in [5]. The flow channel of each membrane module is discretized into finite segments. At each segment, the governing Eqs. (11) – (16) are iteratively solved to calculate the local fluid properties. The numerical calculation procedure is described in detail as follows (right-hand box):

   a. The permeate and membrane wall concentrations, C_p and C_m, and volumetric permeate flux, J_w, are initially guessed.

   b. The trans-membrane osmotic pressure, $\Delta\pi$, and J_w are calculated based on the estimated value of C_m using the film theory model.

c. The preceding procedure is repeated until the error ε between $J_{w,guess}$ and $J_{w,calculated}$ is below a tolerance value of 5×10^{-4}. When returning to the guess step, the calculated value is used as a new guess value.

d. C_m and C_p are recalculated using Eq. (13) once their ε values are below the tolerance. When the ε between the guessed and calculated ones is over the tolerance, a series of previous process is iterated until the ε satisfies the tolerance criterion.

e. The permeate and retentate flow rates, concentrations, and pressures of a membrane module are calculated using Eqs. (14) – (18).

(3) The feed water variables, Q_6, C_6, Q_7, and C_7, are calculated using differential mass balance Eqs. (1) – (4). The obtained values are updated as new input values for those variables to compute the performance for Stage 1 NF and Stage 2 RO at a next time step. A series of the previous steps (2) and (3) are iterated until the variables reach to steady state conditions.

(4) SEC of the 1-2 EERO process is evaluated by calculating the work-rate $\dot{W}$ of ancillary equipment using Eqs. (5) – (10).

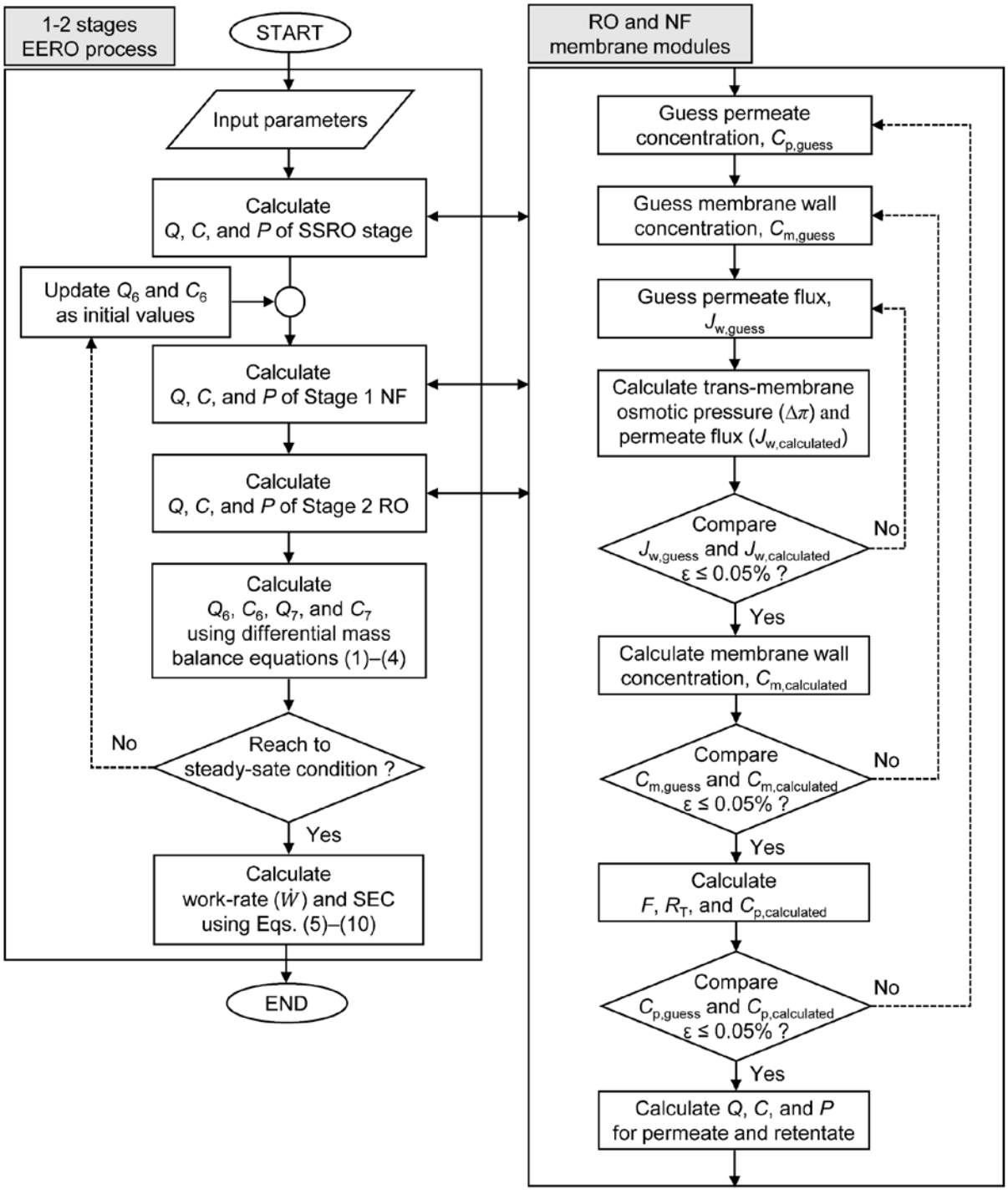

316

317 Fig. 2. Flow chart of the modeling procedure for energy-efficient reverse osmosis (EERO)
318 process.

Table 1 Simulation conditions of 1-2 EERO process.

Parameter	Value	Units
Operating conditions		
Inlet feed flow rate, Q_f	360	m^3/day
Inlet feed pressure [a]		
SSRO stage, P_f	43.5 – 79.8	bar
Stage 2 RO, P_7	10.3 – 59.9 (up to 107.4 [b])	bar
Temperature, T	25	°C
Retentate recycle ratio, R	0 – 0.9	-
Pump efficiency, η_{pump}	0.85	-
Energy recovery device efficiency, η_{ERD}	0.90	-
Feed water properties		
Solute concentration, C_f	35	g/L (NaCl)
Solute diffusivity, D_b	1.51×10^{-9}	m^2/s
Dynamic viscosity, μ	1.0978×10^{-3}	Pa s
Kinematic viscosity, v	9.5×10^{-7}	m^2/s
Module properties [c]		
Spacer thickness, H	7.11 (RO), 8.64 (NF)	10^{-4} m
Spacer porosity, ε_{sp}	0.8	-
Friction coefficient due to spacer, K	7 (RO), 10 (NF)	-
Membrane area/element	41.0 (RO), 37.2 (NF)	m^2
Leaf width, W	0.72 (RO), 0.66 (NF)	m
Leaf length, L	0.92	m
No. of leafs/element, N_L	31	#
No. of elements/module, N_E	8	# (in series)
No. of modules/stage, N_M	1	#
Membrane properties [d]		
Water permeability, L_p	1.739	L/(m^2 h bar)
Solute permeability, P_s	0.064	L/(m^2 h)
Reflection coefficient, σ	1	-

[a] The range of feed pressures to achieve water recoveries of 20 – 60% (SSRO stage) and 20 – 55% (Stage 2 RO) at a retentate recycle ratio of 0.6.

[b] Number highlighted in grey are for purpose of comparison and may not be applicable in practice.

[c] The DOW FILMTEC elements, SW30XLE-440i, NF90-400/34i, and NF270-400/34i, were embedded in the RO and NF modules, respectively.

[d] The properties, listed in this table, include three membrane transport coefficients for SW30XLE-440i [5]. Those of NF90-400/34i and NF270-400/34i were estimated using empirical correlations, which are described in detail in Appendix A.

3. Results and discussion

3.1. Model validation

The accuracy of the developed numerical model was validated under various operating conditions prior to simulating the effect of system variables such as retentate recycle ratio and water recovery on the 1-2 EERO process. Fig. 3 presents the comparisons between the simulated data and the projected data from Reverse Osmosis System Analysis (ROSA) 9 that is a commercial projection software provided by the membrane manufacturer, DOW FILMTEC^{TM}. The result shows a good agreement ($R^2 > 0.97$) of the permeate flow rates and salt passage between the projected data and simulated data for both RO and NF processes. Note that the performance data for each process were collected based on a module design with a single pressure vessel with eight membrane elements (8-inch) for a single-stage configuration within the range of operating conditions in a 1-2 EERO system.

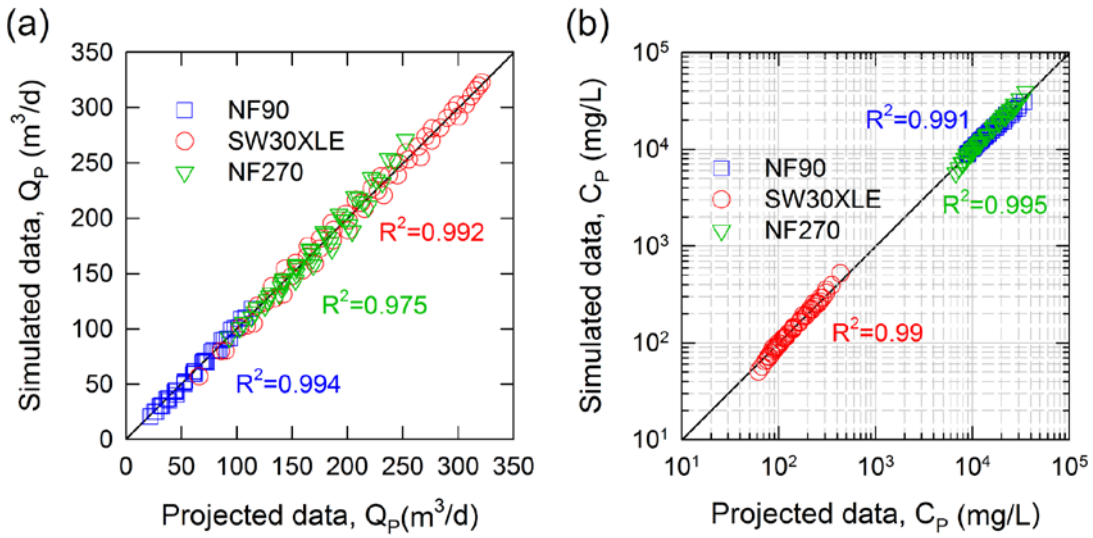

Fig. 3. Comparisons of the projected (x-axis) and simulated (y-axis) data for (a) permeate flow rate and (b) permeate salt concentration. Individual points indicate the performance obtained under various operating conditions as follows: for SW30XLE-440i – feed concentration (10 – 50 g/L at 5 g/L intervals); inlet feed pressure (55 – 80 bar at 5 bar intervals); feed flow rate (360 m^3/d). for NF90-400/34i and NF270-400/34i – feed concentration (50 – 90 g/L at 5 g/L intervals); inlet feed pressure (55 – 75 bar at 5 bar intervals); feed flow rate (190 and 360 m^3/d).

3.2. Dynamic behavior of EERO process

EERO exhibits dynamic behavior of flow rate and concentration at each membrane component until reaching steady state. This dynamic behavior is driven by the mixing process with retentate recycle of Stage 2 RO back to the feed flow of Stage 1 NF. Fig. 4 presents the changes in the flow rate and concentration of the inlet flow to two CMCR stages with time, which was simulated at two different recycle ratios (R = 0 and 0.5). The ratio value of 0 indicates that 100% of Stage 2 retentate flow is recycled to Stage 1, whereas the 0.5 value denotes that the recycle flow is divided equally to Stage 1 and 2, respectively. Generally, the variables shown in Fig. 4 either gradually increased or decreased with time and reached at a steady state briefly in 10 seconds of the system operating time. Note that constant pressures of 18.1 and 30.5 bars were employed for the inlet flow pressure of Stage 2 RO (i.e., P_7) at R = 0 and 0.5, respectively, to keep water recovery of Stage 2 at 50%. The inlet feed flow rate, Q_6, was elevated to ~13% and ~23% by partial (R = 0.5) and complete (R = 0) retentate recycling to Stage 1, respectively (Fig. 4a). In the meantime, the inlet feed flow, Q_7, increased to ~53% at R = 0.5 and 38% at R = 0 due to partial and no retentate recycling to Stage 2, respectively. These would contribute to the OPD reduction for the two CMCR stages because of blending of different concentration streams: lower salinity of the recycled retentate stream (C_5) than the retentate of SSRO stage (C_1); and higher salinity of C_5 than the permeate of Stage 1 (C_4). The inlet flow concentrations of Stage 1 and 2 (C_6 and C_7) at R = 0.5 decreased from 70.0 to 66.2 g/L and increased from 14.8 to 19.2 g/L, respectively (Fig. 4b). Those of Stage 1 and 2 at R = 0 lowered from their initial values to 60.7 and 10.8 g/L, respectively. Such decreases in concentration difference between C_6 and C_7 confirmed that the OPD can be diminished by the retentate recycle and the degree of its change was determined by the recycle ratio. The effect of the retentate recycle is further scrutinized in the subsequent section.

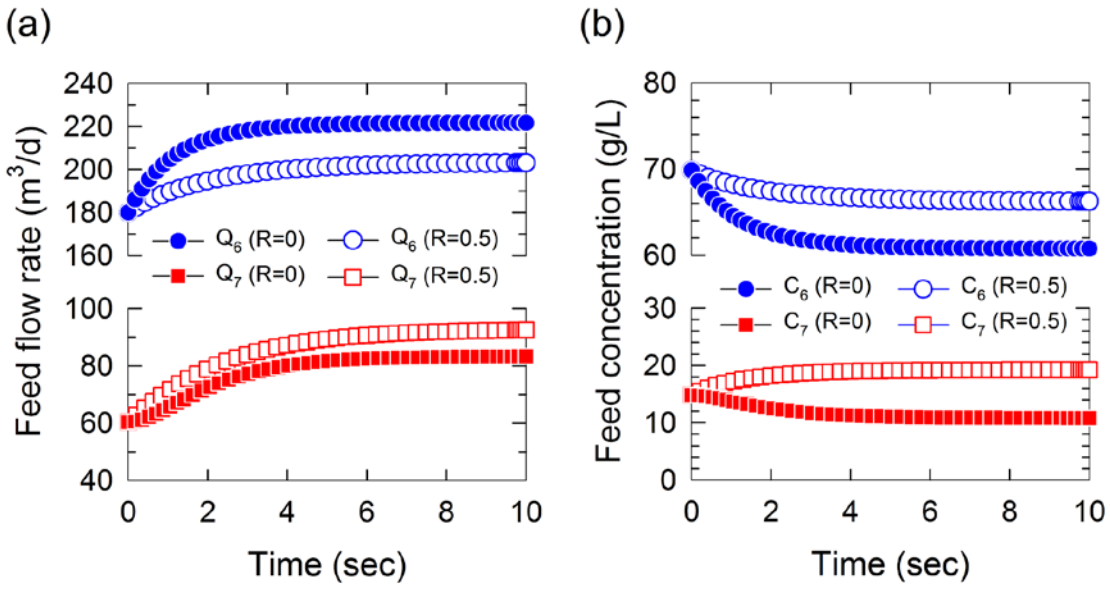

Fig. 4. Impact of retentate recycle on (a) flow rates and (b) concentrations of inlet feed flows of Stage 1 NF and Stage 2 RO in 1-2 EERO process. Simulation was performed under the following operating condition: feed concentration C_f (35 g/L); feed flow rate Q_f (360 m^3/d); SSRO stage recovery (50%); Stage 2 RO recovery (50%); retentate recycle ratio R (0 and 0.5). Each individual stage employs eight membrane elements in a single vessel, and element type is as follows: SSRO stage (SW30XLE-440i); Stage 1 NF (NF90-400/34i); Stage 2 RO (SW30XLE-440i).

3.3. Critical factors affecting EERO process optimization

3.3.1 Retentate recycle

The ultimate goal of EERO application is to minimize operating cost. As described earlier, the retentate recycle is a key feature that diminished OPD for the two CMCR stages. Therefore, it is crucial to scrutinize the optimal recycle ratio for energy minimization. Fig. 5 depicts the profiles of derived and primary energies for the 1-2 EERO process at various retentate recycle ratios under different conditions of Stage 2 RO recovery with a 45% recovery of SSRO stage. It should be noted that derived energy is commonly termed specific energy consumption in membrane processes, so hereinafter it is denoted with SEC. From the result, it was found that such multistage process must be designed with a pairing of recycle ratio and

recovery of Stage 2 RO to reach the optimum SEC when recovery of SSRO is fixed. SEC of the 1-2 EERO can be minimized to ~2.72 kWh/m^3 at which the recycle ratios are 0.8, 0.6, and 0.4 corresponding to 35, 45, and 55% recoveries, respectively. SEC decreased monotonically and slowly as increasing retentate recycle ratio until reaching to the optimal points. Subsequently, abrupt increase in SEC was observed above the optimal points. Interestingly, the minimum energy consumptions were all similar regardless of recovery in Stage 2 RO once reaching to the optimum ratio that was inversely proportional to the Stage 2 RO recovery. The increase in the recovery of Stage 2 RO decreases its outlet flow rate (Q_5), therefore its recycle flow rates to both Stage 1 NF and Stage 2 RO were diminished subsequently. At such condition, decreasing retentate recycle ratio can elevate the inlet flow rate of Stage 1 NF (Q_6) and lessen that of Stage 2 RO (Q_7). Consequently, SEC is reduced by increasing work rate of ERD and decreasing work rates of BP 2 and BP 4. The details of system performance (energy consumption, water recovery, concentration, flow rate, pressure), corresponding to Fig. 5, are provided in Supporting Information Table S1. Additionally, primary energy, corresponding to SEC (technically termed “derived energy”), is depicted in the right axis, which can be converted by multiplying SEC and a conversion factor of 2.13 for SWRO proposed in a recent study [31]. Such primary energy analysis is useful for the cross comparison of assorted desalination methods. SEC of a process should be apportioned to the input primary energy, since it is unable to differentiate the grade of energy supplied to processes accurately [31].

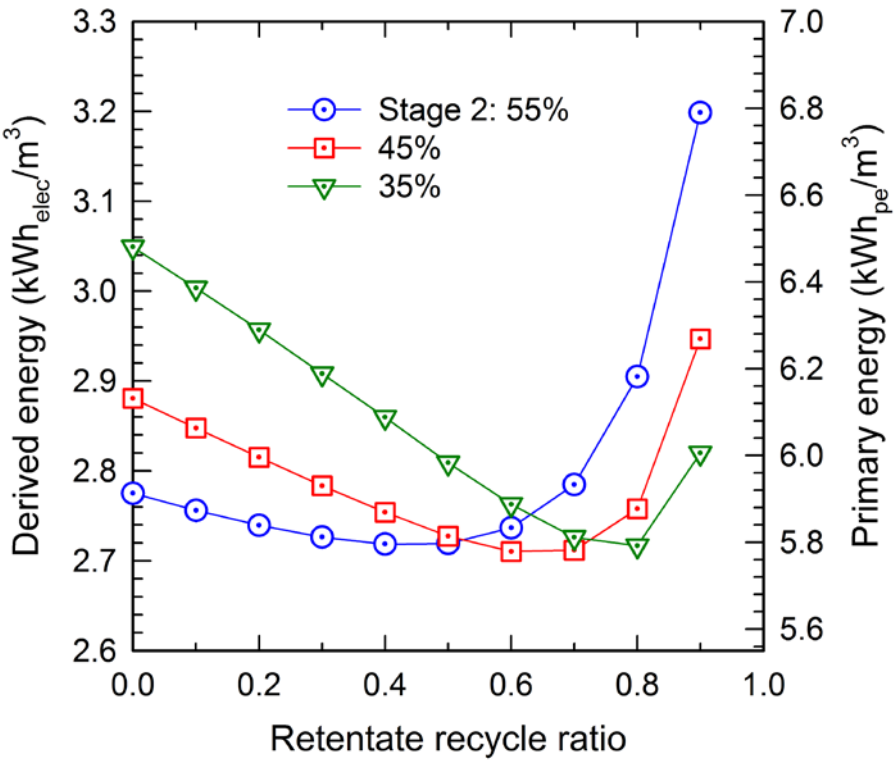

412

413 Fig. 5. Change in (left axis) derived energy and (right axis) primary energy of 1-2 EERO
414 process depending on retentate recycle ratio at different recoveries (35 – 55% at 10% intervals)
415 of Stage 2 RO. Simulation was carried out under the same condition as Table 1. It should be
416 noted that derived energy is commonly termed "specific energy consumption" (SEC).

417

418 ***3.3.2 Water recovery of individual stages***

419 In the preceding section, the impacts of the retentate recycle ratio of Stage 2 RO was
420 investigated. Another important operating parameter for overall energy efficiency is SSRO
421 recovery. Recoveries of SSRO and Stage 2 RO influence their performance interactively,
422 therefore overall performance and energy efficiency. Figs. 6a and 6b depict SEC and overall
423 water recovery of the 1-2 EERO process, respectively. Practical range of water recoveries were
424 tested: 20 – 60% for SSRO stage, ~20 – 45% for Stage 1 NF (see Fig. S1 in Supporting
425 Information), and 20 – 55% for Stage 2 RO. It demonstrates that the system performance was
426 highly reliant on the recovery of individual stages. With the given simulation conditions, SEC
427 varied from 2.52 to 3.42 kWh/m^3 when ERD was embedded in this EERO system (Fig. 6a).

This result shows that the minimum energy can be achieved by adjusting both recoveries of SSRO stage and Stage 2 RO. The SEC value displayed a convex (downward) function of recovery variables in the system. SEC of the system was minimized at 28.3% and 49.0% recoveries for SSRO stage and Stage 2 RO, respectively. Although the both stages' recovery values played important roles in determining SEC, overall recovery was predominantly influenced by SSRO recovery. This is because SSRO stage produces much larger amount of permeate per unit recovery percentage as compared to Stage 2 RO. The minimum SEC value was obtained at a recovery of ~42% for the 1-2 EERO system (Fig. 6b).

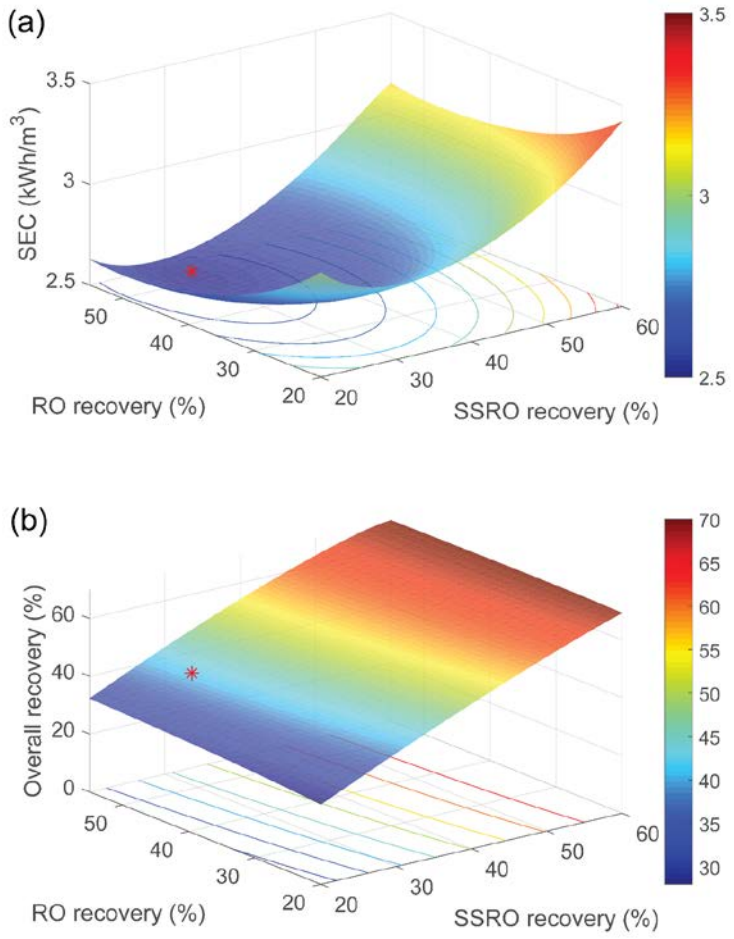

Fig. 6. Comparisons of (a) specific energy consumptions and (b) overall water recoveries under various recovery conditions in SSRO stage and Stage 2 RO in 1-2 EERO process. In the figure, optimal recovery of the system is indicated by a red-colored star (∗) symbol. For simulations, we employed a retentate-recycle ratio R of 0.6, while the other conditions were the same as those of Table 1.

3.3.3 Overall water recovery

When designing a desalination system, it is reasonable to compare conventional SSRO, one of the most widely implemented configuration, with EERO at a same recovery rate. As presented in the preceding section, the performance of seawater desalination systems can be significantly affected by their water recoveries. Therefore, it would be important to compare each membrane configuration at same overall water recoveries. Fig. 7 depicts the SEC profiles for conventional SSRO and 1-2 EERO processes with respect to overall water recovery at a retentate recycle ratio of 0.6. The minimum SEC values, obtained previously for each overall recovery rate (Fig. 6a), were presented. SEC for conventional SSRO and EERO processes showed exponential and concave upward trends, respectively. The SEC for the 1-2 EERO was reduced up to 2.52 kWh/m^3 in the range of 35 – 50%, while conventional SSRO obtained a lower SEC value (2.27 – 2.50 kWh/m^3) in the range of 30 – 50%, but was more significantly augmented for the overall recovery greater than 50%. With such a high recovery, its energy efficiency was more rapidly degraded in comparison with the EERO process. As a result, the 1-2 EERO becomes more energy-efficient than conventional SSRO at above 55% recovery. The 1-2 EERO exhibited 3.1 – 25.1% lower values of SEC at 55 – 69% overall recoveries with TDS concentration of < 220 mg/L in permeate, which was competitive to that of conventional SSRO (Table 2). This result implies that the 1-2 EERO process can be a promising design option for high-recovery desalination, even though it was prone to more pressure drops: 4.6 – 7.4 bars (i.e., a summation of total pressure drops in each individual stages) for 1-2 EERO and 2.2 – 3.6 bars for conventional SSRO depending on overall recovery (30 – 69%). Note that each stage of EERO was below the maximum pressure drop across a pressure vessel of ~3.5 bar (50 psi): 3.3 bar for SSRO stage, 2.2 bar for Stage 1 NF, and 0.5 bar for Stage 2 RO on average. The details of performance (energy consumption, water recovery, concentration, flow

rate, pressure) of the 1-2 EERO, corresponding to Fig. 7, are provided in Supporting Information Table S2.

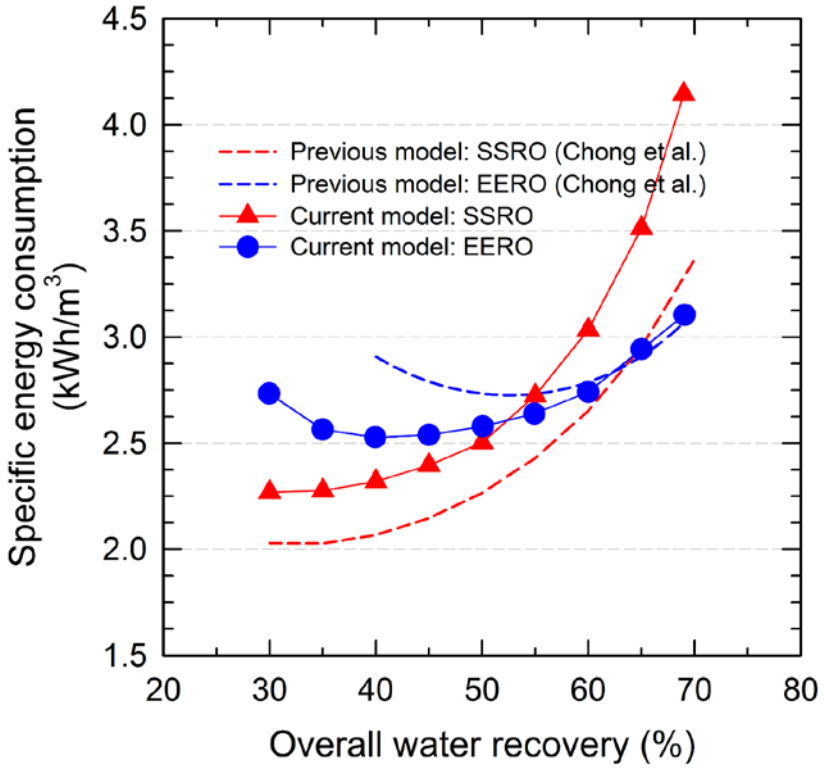

Fig. 7. Comparison of specific energy consumptions (SEC) for conventional SSRO and 1-2 EERO processes in the range of 30 – 69% overall recovery. Note that system performance for the EERO process was simulated within the range of a maximum (acceptable) operating pressure for commercial reverse osmosis membranes. The dotted red and blue color lines indicate SEC profiles of conventional SSRO and 1-2 EERO processes in the previous work [16].

In addition, the preceding result was compared with data from previous analytical models (i.e., dotted lines) [16]. The SEC of SSRO for the previous analytical model was about 14% lower than for the current numerical model. This was likely because of disregard of CP and pressure drop effects have underestimated the SEC. On the other hand, the SEC for the 1-2 EERO of the previous analytical model was higher than that for the current numerical model. This could be attributed to that the 1-2 EERO of this study was optimized regarding to retentate

recycle ratio and recoveries of individual stages. Despite such optimization, an interesting observation was that little/no improvement of the current numerical model in SEC relative to the previous analytical model when an overall recovery was over 50%. This could be explained by the least and excess works of separation (also known as thermodynamic minimum energy and irreversible energy loss, respectively), to which CP and pressure drop effects contribute partly, become more significant in practice, because such limiting factors are greater with a higher recovery. Accordingly, the improved energy (of the current numerical model) was reduced gradually with the recovery, and eventually converged with SEC (of the previous analytical model) at high recovery of > 60%. Nevertheless, a key finding of this result was that the critical recovery (beyond which EERO gives lower SEC relative to conventional SSRO) can be practically shifted from ~65% (the previous analytical model) to ~55% (the current numerical model). This implies that the 1-2 EERO process could be more feasible than expected in the previous assessment.

Furthermore, lower membrane fouling propensity of EERO process can be a major benefit over conventional SSRO stage. In order to achieve a same recovery for both conventional SSRO and 1-2 EERO, the amount of water loaded onto each membrane module will be greater for conventional SSRO. It is known that the extent of fouling is proportional to convective flux of foulants toward membrane surface [32]. Therefore, greater recovery (equivalently, flux) per stage would cause greater extent of fouling. By employing more stages, lower recovery for SSRO stage in EERO configuration can be obtained (Table 2). To be specific, 1-2 EERO process achieved up to 33.3% lower recovery (26.8% on average) for SSRO stage in EERO than conventional SSRO. While EERO is expected to have lower fouling propensity, its demonstration remains as a future study. In terms of membrane fouling, 1-2 EERO process would be best operated at 60% recovery from a practical point of view. This is to ensure the maximum water flux of all elements in the pressure vessel was below the recommended

maximum limit (i.e. 35.7 LMH for seawater pretreated with DOW UF, SDI < 2.5 [33]) (Supporting Information Table S3). To allow higher recovery > 60%, i.e., higher maximum water flux per element, the system needs to consider pretreatment technologies superior to the existing UF.

Table 2. Simulated profiles of water recovery and final product water concentration for conventional SSRO and 1-2 EERO processes with respect to overall recovery [a].

Overall recovery (%)	Conventional SSRO		1-2 EERO [b]		
	Recovery (%)	Permeate concentration (mg/L)	Recovery (%)		Permeate concentration (mg/L)
			SSRO stage	Stage 2 RO	
30	30	217	20.0	33.3	261
35	35	195	22.8	47.8	258
40	40	180	26.9	49.0	237
45	45	170	31.0	53.8	236
50	50	164	36.6	44.1	200
55	55	161	40.7	52.6	217
60	60	158	46.2	51.4	215
65	65	156	53.1	36.9	190
69	69	155	58.6	39.3	210

[a] Numbers highlighted in grey are for purpose of comparison and may not be applicable in practice as either maximum permeate flux or pressure are > 35.7 LMH or > 83 bar, respectively.
[b] Recoveries of individual stages are for conditions of minimum specific energy consumption (SEC) at each overall recovery (shown in Fig. 7).

3.3.4 NF module design

To improve the energy efficiency of 1-2 EERO process, NF stage of the system needs to be designed with membranes with the proper rejection and permeability depending on overall recovery rate. This is because the flow rate, concentration, and applied pressure of Stage 2 inlet stream are significantly influenced by those of Stage 1 outlet (permeate) stream. In this regard, it would be meaningful to identify the effect of NF module designs in Stage 1 on the EERO performance. To attain this end, we evaluated the normalized specific energy consumption (SEC_{norm}) for 1-2 EERO process with 60% overall water recovery, where conventional and internally-staged designs (ISD) were employed for a single pressure vessel of NF stage. Note that the conventional design loaded a pressure vessel with single-type membrane elements, either NF90 or NF270, while both types of membranes were hybridized for ISD (Fig. 8a).

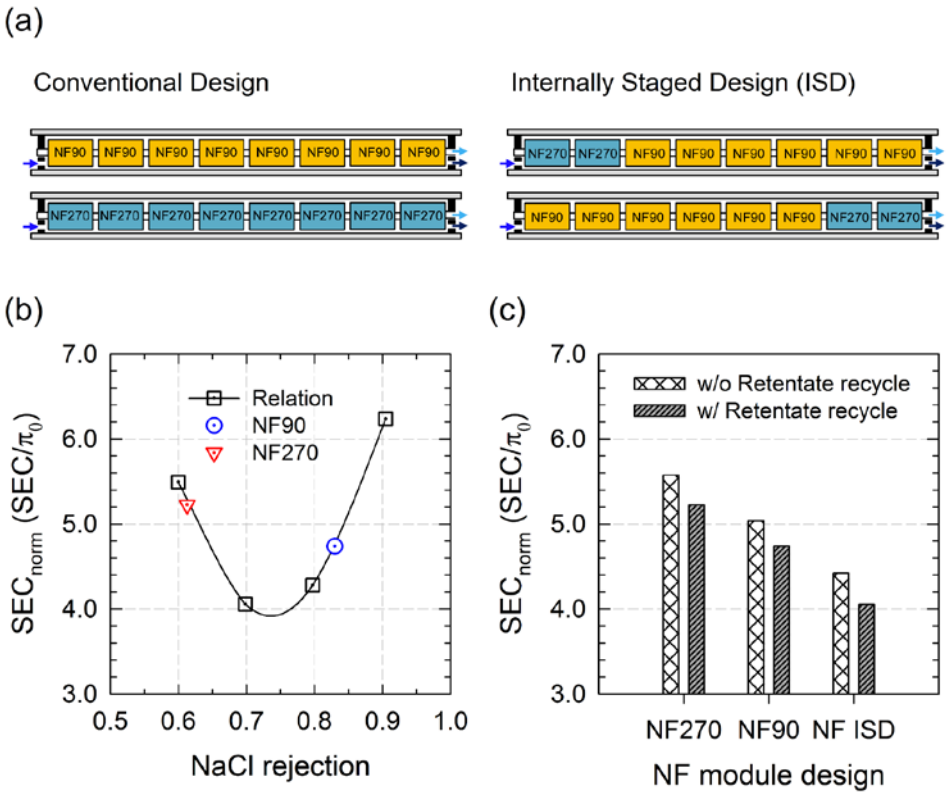

Fig. 8. Comparisons of normalized specific energy consumptions for 1-2 EERO processes with 60% overall water recovery, which have single pressure vessel of (a) four distinct

configurations of NF membrane elements, (b) different salt rejections, and (c) different modular designs in the presence and absence of retentate recycle. NF ISD, one of NF membrane modular designs in this study, denotes is a hybrid configuration of six NF90-400/34i and two NF270-400/34i.

As a preliminary work, first we tested different NF modules that possess salt rejections ranging 60 – 90% at 10% intervals (Fig. 8b). To perform simulations with different salt rejections, the permeability coefficient P_s, a key parameter determining the membrane solute flux, was adjusted in modeling. From Fig. 8b, the lowest SEC_{norm} value for 1-2 EERO process was found at salt rejection of 70% among the designs with the selected rejections. In addition, according to the black solid curve in relation to the selected rejections, a critical range of salt rejection was found to be 70 – 76% where a relatively low value of SEC_{norm} ($\leq$ ~4) can be achieved. SEC_{norm} of 1-2 EERO process was considerably increased when salt rejection was either reduced below 60% or raised above 90% from the optimum at 70%. This result could be explained by the trade-off relationship between permeability and selectivity in polymer membranes. A membrane module with very high rejection for NF stage will have low permeate flow rate, as such the feed flow rate for the subsequent RO stage is excessively reduced. In contrast, although a membrane module with very low rejection can lead to a high feed flow rate for the subsequent RO stage, it also increases the feed concentration for the corresponding stage, thereby a greater pressure is required to attain similar target water recovery.

As means of further optimization of the NF stage, we analyzed SEC_{norm} of the 1-2 EERO process for three cases of NF membrane element configurations with and without retentate recycle (Fig. 8c). ISD can facilitate practical application of optimal rejection of salt to NF stage. As presented in Fig. 8b, the NF90 and NF270 had a salt rejection of 83% and 61%, respectively. The NF ISD, however, acquired the optimum rejection of 70% for NF stage by using six NF90-400/34i and two NF270-400/34i. From Fig. 8c, it was revealed which factor between NF module design and retentate recycle was more sensitive to the EERO system in

561 term of energy reduction. The result showed that SEC_{norm} of NF ISD decreased by averagely
562 18.4% as compared to those of the other configurations (NF90 and NF270). The values of
563 SEC_{norm} depending on the presence and absence of retentate recycle, meanwhile, exhibited <
564 7.0% difference on average for all the designs.

565 Fig. 9 illustrates the profiles of permeate flux in a pressure vessel for individual stages
566 of conventional SSRO and 1-2 EERO processes. The figure demonstrated that the 1-2 EERO
567 process can possess the advantage of mitigating CP and membrane fouling over the
568 conventional processes (Fig. 9a). The two RO stages of the 1-2 EERO maintained the lower
569 level of permeate flux, especially at the lead elements, when compared to the conventional
570 SSRO. With the multi-staged operation, the 1-2 EERO had significantly reduced the fluxes
571 (averagely ~27% and ~76%) of the elements 1 – 5 for SSRO stage and Stage 2 RO, respectively,
572 at the same high overall recovery of 60%. On the other hand, the front element flux for
573 conventional SSRO at 60% recovery has exceeded the maximum recommended limit (i.e. 35.7
574 LMH for seawater pretreated with DOW UF, SDI < 2.5 [33]), thus it is only suitable for typical
575 operating conditions of 40 – 45% recoveries (see Supporting Information Table S3). In addition,
576 the conventional SSRO exhibited the highest degree of the flow imbalance over the vessel as
577 observed in Fig. 9a. The corresponding CP values were reduced by 5.2% and 18.3% for the
578 first element of SSRO stage and Stage 2 RO, respectively, compared to the conventional SSRO.
579 An increase in permeate flux at the lead elements causes a higher retentate concentration,
580 thereby increasing feed concentration to the subsequent tail elements. Therefore, such a high-
581 recovery conventional SSRO would have the potential to aggravate not only organic and
582 colloidal fouling at the lead elements, but also scaling of inorganic substances at the tail
583 elements.

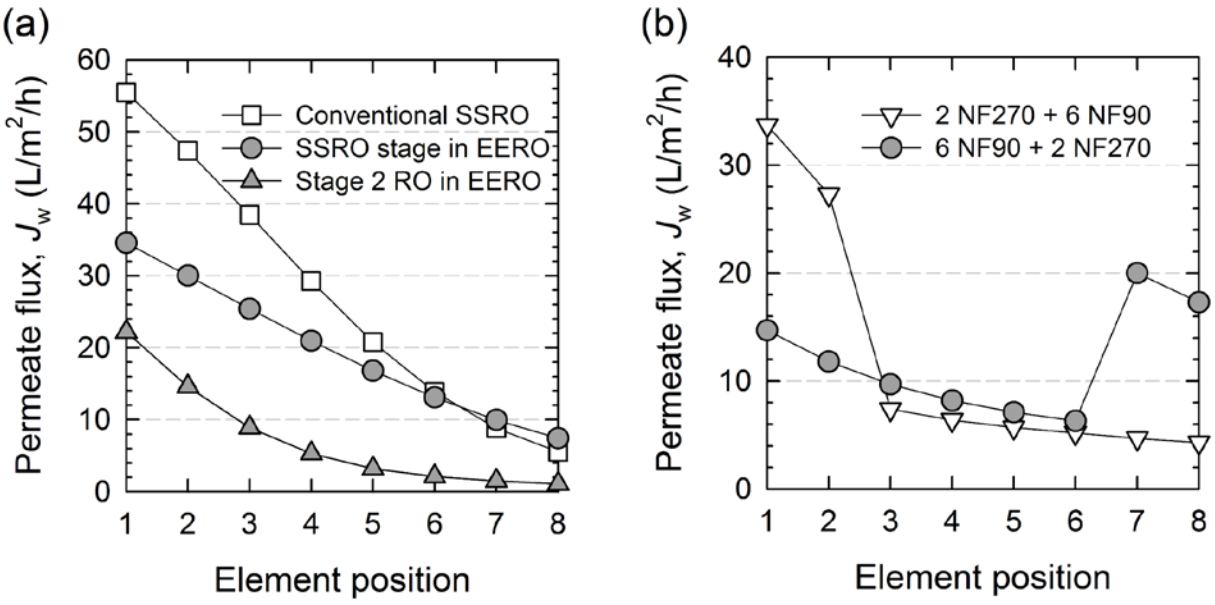

584

585 Fig. 9. Permeate flux of element of (a) RO stage in conventional SSRO and 1-2 EERO
586 processes, and (b) NF stage with ISD in 1-2 EERO processes. The permeate fluxes were
587 simulated at an overall water recovery of 60%.

588

589 The investigation into ISD for NF stage's module could be informative, because the
590 permeate flux profile along the element position can be largely changed depending on how we
591 internally arrange different types of membrane elements within the vessel [5]. In this study, the
592 permeate flux for two different ISDs were evaluated (Fig. 9b): 1) two NF270-400/34i + six
593 NF90-400/34i; 2) six NF90-400/34i + two NF270-400/34i. Note that both element
594 configurations can be considered as a part of ISD options in actual practice, because they
595 attained the water recovery and salt rejection of near the optimum (70%) from their single
596 pressure vessels, under almost similar operating conditions in NF stage. From the result, it was
597 found that the latter configuration was more suitable for NF ISD, since its permeate flux at the
598 first two elements was significantly lower than that of the former. The permeate flux of the
599 latter noticeably increased at the last two tail elements, but this design was still expected to
600 have less fouling potential due to a relatively low level of permeate flux (≤ 20 LMH) over the
601 vessel.

4. Conclusion

This study was primarily aimed at assessing and optimizing the efficiency of a 1-2 EERO process. To this end, the 1-2 EERO process was numerically modeled, and its performance was then predicted under various operating conditions. For practical simulations, we considered performance-limiting factors (i.e., concentration polarization and frictional pressure drop) since these are more significant in a full-scale multistage process than a single-stage one. Overall, new findings of this study are listed as below:

- Retentate recycle flows sufficiently increased the feed flow rates of Stage 1 NF and Stage 2 RO and reduced concentration difference across the membrane, thereby lowering the OPD for CMCR stages. The degree of changes in the feed flow rate and concentration is influenced by the retentate recycle ratio.
- For the 1-2 EERO process, energy efficiency is highly reliant on retentate recycle ratio. The recycle ratio, particularly for 45% recovery of SSRO stage was optimum at 0.8, 0.6, and 0.4 corresponding to 35, 45, and 55% recoveries of Stage 2 RO, respectively. In addition, SEC increased significantly under the condition smaller and greater than the optimum ratio. This could be attributed to that such a ratio has an influence on the work rate done by the ancillary equipment such as ERD and BPs.
- We found an optimal water recovery to minimize SEC of the 1-2 EERO process in the presence of ERD: an overall recovery of ~42% with a recovery of 28.3% and 49% for SSRO stage and Stage 2 RO, respectively.
- The 1-2 EERO process can outperform a conventional SSRO process for high overall recovery of $\geq$ 55% with a decent quality (< 220 mg/L) of the final product

water; The EERO process optimized here not only decreased SEC at high water recovery, but also yielded lower potentials of membrane fouling and CP due to reduced permeate flux in the lead elements in SSRO stage and Stage 2 RO.

- NF module design had a larger impact on the improvement in energy efficiency for the 1-2 EERO process, than the retentate recycle. The NF stage, therefore, needed be designed in accordance with a criterion of the optimum salt rejection for target recovery: for overall recovery of 60%, a NF module of 70% salt rejection had the lowest SEC_{norm} among the ones in the range of 60 – 90% salt rejections. In this regard, ISD was useful for effectively designing the NF module, because it could be adjusted to the optimum rejection through a hybrid configuration of different NF membranes in a pressure vessel.

The numerical model developed here can be a reliable assessment tool, which can help process engineers' decision-making for design and operation of a 1-2 EERO system. In addition, it is also expected that the proposed modeling approach would be a good reference for a modeling of a multi-stage membrane process with CMCR. Lastly, as shown in the work, the NF stage plays a critical role in determining the efficiency of the EERO system. Thus, robust NF membranes such as greater maximum operating pressure (i.e. most of current commercial NF membranes are limited to 41 bar) and wider rejection range are required.

Acknowledgments

This research grant was supported by the Singapore National Research Foundation under its Environment and Water Research Program and administered by PUB. The Singapore Membrane Technology Center, Nanyang Environment and Water Research Institute, Nanyang Technological University is supported by the Economic Development Board of Singapore.

650

651 **Nomenclature**

C^{p}_{module}	permeate concentration of a single membrane module (mg/L)
c	concentration (mg/L)
D	diffusion coefficient of solute (m^2/s)
d_h	hydraulic diameter (m)
H	channel height (m)
J_s	salt flux ($kg/m^2\,s$)
J_w	permeate flux (m/s)
K	friction coefficient
k	mass transfer coefficient (m/s)
L	channel length (m)
L_p	water permeability coefficient ($L/m^2\,h\,bar$)
M	molecular weight (g/mol)
N	total number
N_{ion}	ionization number of the solution
P	inlet and outlet flow pressure (bar)
p	pressure (bar)
P_s	salt permeability coefficient ($L/m^2\,h$)
Q	inlet and outlet volumetric flow rate (m^3/d)
Q^{p}_{module}	permeate flow rate of a single membrane module (m^3/d)
R_g	ideal gas constant ($cm^3\,bar/mol\,K$)
Re	Reynolds number
Sc	Schmidt number
SEC	specific energy consumption ($kW\,h/m^3$)

Sh	Sherwood number
T	absolute temperature (K)
TL	total length of flow channel in a pressure vessel (m)
u	cross-flow velocity (m/s)
V	volume (m^3)
W	channel width (m)
$\dot{W}$	rate of work done (KJ/d)
x	coordinate in channel length direction
Y	water recovery

Greek Symbols

ε_{sp}	effective porosity of flow channel created by feed spacer
η	equipment efficiency
μ	dynamic viscosity (Pa s)
ν	kinematic viscosity (m^2/s)
π	osmotic pressure (bar)
σ	reflection coefficient

Subscripts and Superscripts

BPs	booster pumps
b	bulk
E	membrane element
ERD	energy recovery device
elec	electricity
f	feed flow to SSRO stage
HPP	high pressure pump
L	membrane leaf

M	membrane module
m	membrane wall (active layer surface)
NF	nanofiltration
norm	normalized to the feed osmotic pressure
overall	total quantity
p	permeate
pe	primary energy
RO	reverse osmosis
SSRO	single-stage reverse osmosis
STG2	stage 2
s	salt
sw	saltwater
w	water
0	influent (feed)

References

[1] S. Loeb, S. Sourirajan, Sea water demineralization by means of an osmotic membrane, in, ACS Publications, 1962.

[2] M. Elimelech, W.A. Phillip, The future of seawater desalination: energy, technology, and the environment, science, 333 (2011) 712-717.

[3] G.M. Geise, H.B. Park, A.C. Sagle, B.D. Freeman, J.E. McGrath, Water permeability and water/salt selectivity tradeoff in polymers for desalination, Journal of Membrane Science, 369 (2011) 130-138.

[4] M. Wilf, C. Bartels, Optimization of seawater RO systems design, Desalination, 173 (2005) 1-12.

[5] K. Jeong, M. Park, S.J. Ki, J.H. Kim, A systematic optimization of Internally Staged Design (ISD) for a full-scale reverse osmosis process, Journal of Membrane Science, (2017).

[6] S. Lin, M. Elimelech, Kinetics and energetics trade-off in reverse osmosis desalination with different configurations, Desalination, 401 (2017) 42-52.

[7] T.H. Chong, S.-L. Loo, W.B. Krantz, Energy-efficient reverse osmosis desalination process, Journal of Membrane Science, 473 (2015) 177-188.

[8] L.F. Greenlee, D.F. Lawler, B.D. Freeman, B. Marrot, P. Moulin, Reverse osmosis desalination: water sources, technology, and today's challenges, Water research, 43 (2009) 2317-2348.

[9] N. Kishizawa, K. Tsuzuki, M. Hayatsu, Low pressure multi-stage RO system developed in “Mega-ton Water System” for large-scaled SWRO plant, Desalination, 368 (2015) 81-88.

[10] L. Chekli, S. Phuntsho, J.E. Kim, J. Kim, J.Y. Choi, J.-S. Choi, S. Kim, J.H. Kim, S. Hong, J. Sohn, A comprehensive review of hybrid forward osmosis systems: Performance, applications and future prospects, Journal of Membrane Science, 497 (2016) 430-449.

[11] A. Altaee, A. Sharif, Pressure retarded osmosis: advancement in the process applications for power

generation and desalination, Desalination, 356 (2015) 31-46.
[12] J. Ren, J.R. McCutcheon, A new commercial thin film composite membrane for forward osmosis, Desalination, 343 (2014) 187-193.
[13] S. Lin, M. Elimelech, Staged reverse osmosis operation: Configurations, energy efficiency, and application potential, Desalination, 366 (2015) 9-14.
[14] D.M. Warsinger, E.W. Tow, K.G. Nayar, L.A. Maswadeh, Energy efficiency of batch and semi-batch (CCRO) reverse osmosis desalination, Water research, 106 (2016) 272-282.
[15] J.R. Werber, A. Deshmukh, M. Elimelech, Can batch or semi-batch processes save energy in reverse-osmosis desalination?, Desalination, 402 (2017) 109-122.
[16] T.H. Chong, S.-L. Loo, A.G. Fane, W.B. Krantz, Energy-efficient reverse osmosis desalination: effect of retentate recycle and pump and energy recovery device efficiencies, Desalination, 366 (2015) 15-31.
[17] G. Artuğ, Modelling and simulation of nanofiltration membranes, Cuvillier Verlag, 2007.
[18] A. Zhu, P.D. Christofides, Y. Cohen, Minimization of energy consumption for a two-pass membrane desalination: effect of energy recovery, membrane rejection and retentate recycling, Journal of Membrane Science, 339 (2009) 126-137.
[19] X.-L. Wang, T. Tsuru, S.-i. Nakao, S. Kimura, The electrostatic and steric-hindrance model for the transport of charged solutes through nanofiltration membranes, Journal of Membrane Science, 135 (1997) 19-32.
[20] O. Kedem, A. Katchalsky, Thermodynamic analysis of the permeability of biological membranes to non-electrolytes, Biochimica et biophysica Acta, 27 (1958) 229-246.
[21] M. Soltanieh, W.N. GILL', Review of reverse osmosis membranes and transport models, Chemical Engineering Communications, 12 (1981) 279-363.
[22] A. Ahmad, M. Chong, S. Bhatia, Mathematical modeling and simulation of the multiple solutes system for nanofiltration process, Journal of Membrane Science, 253 (2005) 103-115.
[23] W.R. Bowen, J.S. Welfoot, Modelling the performance of membrane nanofiltration—critical assessment and model development, Chemical Engineering Science, 57 (2002) 1121-1137.
[24] X.-L. Wang, T. Tsuru, M. Togoh, S.-i. Nakao, S. Kimura, Evaluation of pore structure and electrical properties of nanofiltration membranes, Journal of chemical engineering of Japan, 28 (1995) 186-192.
[25] W. Zhou, L. Song, T.K. Guan, A numerical study on concentration polarization and system performance of spiral wound RO membrane modules, Journal of Membrane Science, 271 (2006) 38-46.
[26] K. Spiegler, O. Kedem, Thermodynamics of hyperfiltration (reverse osmosis): criteria for efficient membranes, Desalination, 1 (1966) 311-326.
[27] W.F. Blatt, A. Dravid, A.S. Michaels, L. Nelsen, Solute polarization and cake formation in membrane ultrafiltration: causes, consequences and control techniques, Membrane science and technology, 47 (1970).
[28] G. Schock, A. Miquel, Mass transfer and pressure loss in spiral wound modules, Desalination, 64 (1987) 339-352.
[29] K.L. Chen, L. Song, S.L. Ong, W.J. Ng, The development of membrane fouling in full-scale RO processes, Journal of Membrane Science, 232 (2004) 63-72.
[30] E.M. Hoek, J. Allred, T. Knoell, B.-H. Jeong, Modeling the effects of fouling on full-scale reverse osmosis processes, Journal of Membrane Science, 314 (2008) 33-49.
[31] K.C. Ng, M.W. Shahzad, H.S. Son, O.A. Hamed, An exergy approach to efficiency evaluation of desalination, Applied Physics Letters, 110 (2017) 184101.
[32] M. Park, J. Lee, C. Boo, S. Hong, S.A. Snyder, J.H. Kim, Modeling of colloidal fouling in forward osmosis membrane: Effects of reverse draw solution permeation, Desalination, 314 (2013) 115-123.
[33] Dow Water & Process Solutions, FILMTEC™ Reverse Osmosis Membranes Technical Manual, in.
[34] P. Eriksson, Water and salt transport through two types of polyamide composite membranes, Journal of Membrane Science, 36 (1988) 297-313.
[35] N. Hilal, H. Al-Zoubi, A.W. Mohammad, N. Darwish, Nanofiltration of highly concentrated salt solutions up to seawater salinity, Desalination, 184 (2005) 315-326.

Appendix A. Estimation of intrinsic transport properties of a commercial NF membrane

From the literature [24, 34, 35], it was reported that the membrane transport coefficients of NF membranes are strongly dependent on the feed concentration of electrolyte solutions, due to electrostatic interactions between the charged membrane and ions in the solution [34]. They experimentally confirmed the concentration-dependent relations of those parameters, and further demonstrated it theoretically using membrane transport models. However, it is challenging to fully describe the behavior of those parameters for various NF membranes with the wide range of feed concentrations using simple mathematical equations. Therefore, we believe that the empirical relationship we obtained here (Fig. A1) is sufficient to accurately estimate the values of the transport coefficients for commercial NF membranes, NF90 and NF270. It can further allow a successful prediction of the NF module performance in Stage 1 for high feed concentrations as saline as seawater reverse osmosis (SWRO) brine.

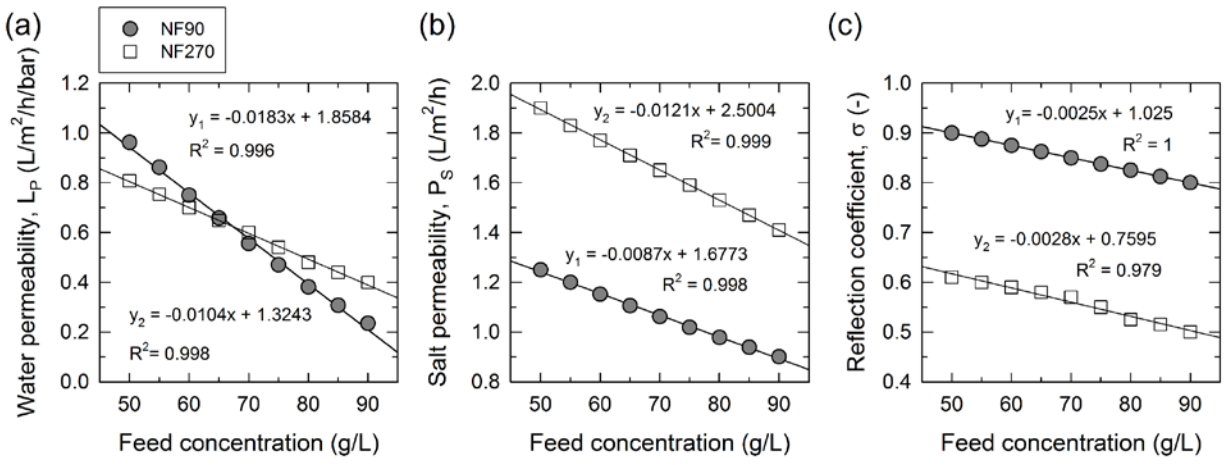

Fig. A1. Empirical linear correlations between the feed solute concentration and intrinsic transport properties for commercial nanofiltration membranes.

To obtain the empirical linear equations (shown in Fig. A1), we numerically estimated

747 the values of the water and salt permeability coefficients (L_p and P_s) and the reflection
748 coefficient (σ) by fitting these parameters versus the feed concentration. The value of each
749 individual parameter at a single point of the feed concentration was computed by a best fitting
750 method to minimize an error value (an average error of 2.0%) between the simulated and
751 projected data. Specifically, the ROSA9 software evaluated the permeate flow rates and salt
752 concentrations of the NF90 and NF270 membranes. These performance data were obtained for
753 feed concentrations of 50 – 90 g/L at 5 g/L intervals with a feed pressure of 65 bar, which is
754 normal operating conditions for NF module in the 1-2 EERO process. The parameters L_p, P_s,
755 and σ were computed using a series of Eqs. (11) – (18) and the performance data obtained at
756 an given condition. With the empirical linear correlations, the developed model provided
757 accurate predictions of permeate flow rates and permeate concentrations of a single membrane
758 module under various conditions of the feed concentration and pressure (see Fig. 3).